

University of Wollongong

Research Online

Faculty of Science, Medicine and Health -
Papers: part A

Faculty of Science, Medicine and Health

1-1-2014

Recent Northern Hemisphere stratospheric HCl increase due to atmospheric circulation changes

Emmanuel Mahieu
University of Liege

M P. Chipperfield
University of Leeds

Justus Notholt
University of Bremen

T Reddmann
Institute for Meteorology and Climate Research

J Anderson
Hampton University

See next page for additional authors. <https://ro.uow.edu.au/smhpapers>



Part of the [Medicine and Health Sciences Commons](#), and the [Social and Behavioral Sciences Commons](#)

Recommended Citation

Mahieu, Emmanuel; Chipperfield, M P.; Notholt, Justus; Reddmann, T; Anderson, J; Bernath, Peter; Blumenstock, Thomas; Coffey, M T.; Dhomse, S S.; Feng, W; Franco, B; Froidevaux, L; Griffith, D W. T; Hannigan, J W.; Hase, Frank; Hossaini, R; Jones, Nicholas; Morino, Isamu; Murata, I; Nakajima, H; Palm, M; Paton-Walsh, Clare; Russell III, J M.; Schneider, Matthias; Servais, C; Smale, D; and Walker, K, "Recent Northern Hemisphere stratospheric HCl increase due to atmospheric circulation changes" (2014). *Faculty of Science, Medicine and Health - Papers: part A*. 2359.
<https://ro.uow.edu.au/smhpapers/2359>

Research Online is the open access institutional repository for the University of Wollongong. For further information contact the UOW Library: research-pubs@uow.edu.au

Recent Northern Hemisphere stratospheric HCl increase due to atmospheric circulation changes

Abstract

The abundance of chlorine in the Earth's atmosphere increased considerably during the 1970s to 1990s, following large emissions of anthropogenic long-lived chlorine-containing source gases, notably the chlorofluorocarbons. The chemical inertness of chlorofluorocarbons allows their transport and mixing throughout the troposphere on a global scale¹, before they reach the stratosphere where they release chlorine atoms that cause ozone depletion². The large ozone loss over Antarctica³ was the key observation that stimulated the definition and signing in 1987 of the Montreal Protocol, an international treaty establishing a schedule to reduce the production of the major chlorine- and bromine-containing halocarbons. Owing to its implementation, the near-surface total chlorine concentration showed a maximum in 1993, followed by a decrease of half a per cent to one per cent per year⁴, in line with expectations. Remote-sensing data have revealed a peak in stratospheric chlorine after 1996⁵, then a decrease of close to one per cent per year^{6, 7}, in agreement with the surface observations of the chlorine source gases and model calculations⁷. Here we present ground-based and satellite data that show a recent and significant increase, at the 2σ level, in hydrogen chloride (HCl), the main stratospheric chlorine reservoir, starting around 2007 in the lower stratosphere of the Northern Hemisphere, in contrast with the ongoing monotonic decrease of near-surface source gases. Using model simulations, we attribute this trend anomaly to a slowdown in the Northern Hemisphere atmospheric circulation, occurring over several consecutive years, transporting more aged air to the lower stratosphere, and characterized by a larger relative conversion of source gases to HCl. This short-term dynamical variability will also affect other stratospheric tracers and needs to be accounted for when studying the evolution of the stratospheric ozone layer.

Disciplines

Medicine and Health Sciences | Social and Behavioral Sciences

Publication Details

Mahieu, E., Chipperfield, M. P., Notholt, J., Reddmann, T., Anderson, J., Bernath, P. F., Blumenstock, T., Coffey, M. T., Dhomse, S. S., Feng, W., Franco, B., Froidevaux, L., Griffith, D. W. T., Hannigan, J. W., Hase, F., Hossaini, R., Jones, N. B., Morino, I., Murata, I., Nakajima, H., Palm, M., Paton-Walsh, C., Russell III, J. M., Schneider, M., Servais, C., Smale, D. & Walker, K. A. (2014). Recent Northern Hemisphere stratospheric HCl increase due to atmospheric circulation changes. *Nature*, 515 (7525), 104-107.

Authors

Emmanuel Mahieu, M P. Chipperfield, Justus Notholt, T Reddmann, J Anderson, Peter Bernath, Thomas Blumenstock, M T. Coffey, S S. Dhomse, W Feng, B Franco, L Froidevaux, D W. T Griffith, J W. Hannigan, Frank Hase, R Hossaini, Nicholas Jones, Isamu Morino, I Murata, H Nakajima, M Palm, Clare Paton-Walsh, J M. Russell III, Matthias Schneider, C Servais, D Smale, and K Walker

1 Recent northern hemisphere hydrogen chloride increase
2 due to atmospheric circulation change

3 E. Mahieu¹, M.P. Chipperfield², J. Notholt³, T. Reddman⁴, J. Anderson⁵, P.F. Bernath^{6,7},
4 T. Blumenstock⁴, M.T. Coffey⁸, S. Dhomse², W. Feng², B. Franco¹, L. Froidevaux⁹,
5 D.W.T. Griffith¹⁰, J. Hannigan⁸, F. Hase⁴, R. Hossaini², N.B. Jones¹⁰, I. Morino¹¹,
6 I. Murata¹², H. Nakajima¹¹, M. Palm³, C. Paton-Walsh¹⁰,
7 J.M. Russell III⁵, M. Schneider⁴, C. Servais¹, D. Smale¹³, K.A. Walker^{14,15}

8

9 **Affiliations**

- 10 1. Institute of Astrophysics and Geophysics, University of Liège, Belgium
11 2. National Centre for Atmospheric Science, School of Earth and Environment,
12 University of Leeds, Leeds, U.K.
13 3. Department of Physics, University of Bremen, Germany
14 4. Karlsruhe Institute of Technology (KIT), Institute for Meteorology and Climate
15 Research (IMK-ASF), Karlsruhe, Germany
16 5. Department of Atmospheric and Planetary Science, Hampton University,
17 Hampton, VA, USA
18 6. Department of Chemistry & Biochemistry, Old Dominion University, Norfolk,
19 VA, USA
20 7. Department of Chemistry, University of York, York, U.K.
21 8. National Center for Atmospheric Research, Boulder, CO, USA
22 9. Jet Propulsion Laboratory, California Institute of Technology, Pasadena, CA,
23 USA
24 10. School of Chemistry, University of Wollongong, Wollongong, Australia
25 11. National Institute for Environmental Studies (NIES), Tsukuba, Japan
26 12. Graduate School of Environmental Studies, Tohoku University, Japan
27 13. National Institute of Water and Atmospheric Research (NIWA), Lauder, New
28 Zealand
29 14. Department of Physics, University of Toronto, Toronto, ON, Canada
30 15. Department of Chemistry, University of Waterloo, Waterloo, ON, Canada

31 The abundance of chlorine in the Earth's atmosphere increased considerably during the
32 1970s-1990s, following large emissions of anthropogenic long-lived chlorine-containing
33 source gases, notably the chlorofluorocarbons (CFCs). The chemical inertness of CFCs
34 allows their transport and mixing throughout the troposphere on a global scale¹, before
35 they reach the stratosphere where they release chlorine atoms that cause ozone depletion².
36 The large ozone loss over Antarctica³ was the key observation which stimulated the
37 definition and signing of the Montreal Protocol in 1987, an international treaty
38 establishing a schedule to reduce the production of the major chlorine- and bromine-
39 containing halocarbons. Owing to its implementation, the near-surface total chlorine
40 concentration showed a maximum in 1993, followed by a decrease of 0.5-1 %/yr⁴, in line
41 with expectations. Remote-sensing data have revealed a peak in stratospheric chlorine
42 after 1996⁵, then a decrease at rates close to -1%/yr^{6,7}, in agreement with the surface
43 observations of the chlorine source gases and model calculations⁷. Here we present
44 ground-based and satellite data which show a recent and significant increase in hydrogen
45 chloride (HCl), the main stratospheric chlorine reservoir, starting around 2007 in the
46 northern hemisphere (NH) lower stratosphere, contrasting with the ongoing monotonic
47 decrease of near-surface source gases. Using model simulations we attribute this trend
48 anomaly to a slowdown in the NH atmospheric circulation, occurring over a few
49 consecutive years, transporting more aged air to the lower stratosphere, characterized by
50 a larger relative conversion of source gases to HCl. This short-term dynamical variability
51 will also affect other stratospheric tracers and needs to be accounted for when studying
52 the evolution of the stratospheric ozone layer.

53 Decomposition of chlorine-containing source gases (SG_{Cl}) in the stratosphere produces
54 HCl, the largest reservoir of chlorine^{8,9}. Here we investigate recent trends in atmospheric
55 HCl using observations from eight NDACC-FTIR ground-based stations (from 79°N to
56 45°S, Network for the Detection of Atmospheric Composition Change-Fourier Transform
57 InfraRed instruments, see <http://www.ndacc.org>). Figure 1a shows the HCl total columns
58 for Jungfraujoch (47°N; red squares) together with the evolution of the total tropospheric
59 chlorine (blue curve) over the last three decades. The lower panels (b-d) focus on the
60 recent HCl changes above Ny-Ålesund (79°N) and two mid-latitude stations,
61 Jungfraujoch (zoom of Fig 1a) and Lauder (45°S). While at the southern hemisphere (SH)
62 station we find a continuous decrease of HCl since 2001, both NH sites show an overall
63 HCl decline, more rapid around 2004, followed by an increase from 2007 onwards. In
64 order to quantify the column changes at all sites, we used a bootstrap resampling
65 statistical tool¹⁰ involving a linear component and accounting for the strong seasonal
66 modulations present in the data sets. Figure 2 displays for the eight NDACC sites the
67 relative annual HCl rates of change for the 1997-2007 and 2007-2011 time periods, using
68 either the 1997.0 or 2007.0 computed column as reference. For the 1997-2007 time
69 interval, we determine consistent and significant HCl decreases at all NH sites, with mean
70 relative changes ranging from -0.7 to -1.5%/yr. In the SH, column changes are not
71 significant at the 2- σ level. For 2007-2011, mean relative column growths of 1.1 to
72 3.4%/yr are derived for all NH sites while negative or undefined rates are observed for
73 Wollongong and Lauder in the SH.

74 In order to corroborate these findings with independent data, and to get information on
75 the altitude range where these changes occur, we included the GOZCARDS^{11,12} satellite

76 data set (Global OZone Chemistry And Related Datasets for the Stratosphere; v1.1),
77 which merges observations by the HALOE¹³ (HALogen Occultation Experiment; v19),
78 ACE-FTS¹⁴ (Atmospheric Chemistry Experiment-Fourier Transform Spectrometer; v2.2)
79 and Aura/MLS¹⁵ (Microwave Limb Sounder; v3.3) instruments. Partial columns were
80 computed between 100 and 10 hPa, considering the zonal monthly mean mixing ratio
81 time series available for the whole time interval in the 70-80°N, 60-70°N, 40-50°N, 30-
82 40°N, 20-30°N, 30-40°S and 40-50°S latitudinal bands. These partial columns typically
83 span the 16 to 31 km altitude range, i.e. the region with maximum HCl concentration and
84 to which the FTIR measurements are most sensitive⁵. Corresponding rates of change are
85 also displayed in Figure 2. For 1997-2007, there is excellent agreement in the NH
86 between the satellite and the six NDACC-FTIR trends determined above. In the SH,
87 GOZCARDS reveals statistically significant decreases of HCl while the FTIR time series
88 suggest stable columns at the 2- σ level. For 2007-2011, the ACE-FTS and Aura/MLS
89 merged data confirm the upward FTIR trends in the northern hemisphere. Figure 3
90 illustrates this, showing satellite monthly means (red dots) for 30-60°N and 30-60°S, at
91 46 and 7 hPa, together with a linear fit to the data for both time periods. Clearly, the HCl
92 increase is confined to the NH lower stratosphere.

93 As HCl is the main final product of the decomposition of any SG_{Cl}, we need to verify that
94 its rise after 2007 does not result from the significant contribution of new unknown
95 sources of chlorine whose emissions occur predominantly in the NH, not monitored by
96 the in situ networks, and unregulated by the Montreal Protocol, its Amendments and
97 Adjustments. Indeed, such SG_{Cl} species have been recently identified¹⁶ although in that

98 case, their contribution to the HCl upturn can be ruled out given their very low
99 concentrations.

100 We have used results from two state-of-the-art 3-D chemical transport model SLIMCAT⁷
101 and KASIMA⁷ to interpret the recent HCl increase. Both models performed a standard
102 simulation using surface source gas mixing ratios from the WMO A1 (World
103 Meteorological Organisation; 2010) emission scenario⁴ and were forced using ERA-
104 Interim meteorological fields¹⁷ from the European Centre for Medium-Range Weather
105 Forecasts (ECMWF). The key results for HCl trends from both models agree. Here we
106 show data from the SLIMCAT runs; corresponding results from KASIMA are shown in
107 the Extended Data Figures 1 to 4. To study the impact of atmospheric dynamics, an
108 additional SLIMCAT run (S2000) used constant 2000 meteorological forcing, from 2000
109 onwards. Running averages for both SLIMCAT simulations are reproduced in panels b-d
110 of Figure 1. For the three sites, run S2000 (yellow curve) predicts an overall HCl
111 decrease while the standard run (green squares) reproduces the observed and distinct
112 evolution prevailing in both hemispheres, after correction of a constant low-bias of ~7%
113 in the NH simulations. The total column changes characterizing the model data sets are
114 displayed in Figure 2. The model runs predict significant decreases in HCl for the 1997-
115 2007 reference period at all sites and there is an overall agreement within the error bars
116 for the amplitude of the signals between the model and the observations. Regarding the
117 2007-2011 time period, the SLIMCAT time series are characterized by positive trends
118 from Ny-Ålesund (79°N) to Tsukuba (36°N), by significant decreases for the SH stations,
119 and no significant change for the near-tropical site of Izana (28°N). The S2000 sensitivity
120 run does not produce the HCl trend reversal and, instead, indicates declines at all sites.

121 The agreement between measurement and model demonstrates that the HCl increase after
122 2007 is not caused by new, unidentified chlorine sources, or by underestimates in
123 emissions of known SG_{Cl} species, as these are used as model input. The model-
124 observation agreement also shows that there is a good understanding of the chemistry
125 which converts source gases to HCl. The difference between the HCl trends forecasted by
126 the two SLIMCAT runs, i.e. a significant increase for northern high- and mid-latitudes or
127 a constant decrease below $30^{\circ}N$, establishes that changes in the atmospheric circulation
128 cause the recent HCl increase, since only the meteorological fields adopted from 2000
129 onwards differ between the two runs. To diagnose these circulation changes, we
130 examined age-of-air maps produced by the standard SLIMCAT run. They reveal a slower
131 circulation in the NH lower stratosphere after 2005-2006, with older air characterized by
132 a larger relative conversion of the SG_{Cl} into HCl. Figure 4b shows the age-of-air change
133 between 2005-2006 and 2010-2011. Older air by up to 0.4 yr is found around 20-25 km
134 altitude in a broad range of NH latitudes, in a region where the mean age-of-air is
135 typically about 3 years. There is an obvious correlation with the evolution of the HCl
136 concentrations over the same time period (Fig 4a) which exhibits a very similar pattern
137 and hemispheric asymmetry. Time series of mean age-of-air near 50 hPa above Ny-
138 Ålesund, Jungfraujoch and Lauder are displayed in panel c. The 3-year running means
139 (black curves) indicate a progressive slowdown of the NH stratospheric circulation after
140 2005-2006. For Lauder, a fairly constant circulation speedup occurs from 2000 onwards.
141 These changes are significant, with NH air aging by 3-4 weeks/yr after 2005, compared
142 to ~ 1 week/yr before. For Lauder, the mean age-of-air change during the last decade is
143 calculated to be -2 weeks/yr. Other important factors such as the details of specific

144 transport pathways, which lead to a given mean age-of-air, also affect the conversion rate
145 of the source gases to HCl¹⁸. These pathways are simulated by the model but not revealed
146 by the simple diagnostic of mean age-of-air. The slower NH circulation occurring over a
147 few years after 2005-2006 seems to contrast with the speedup of the Brewer-Dobson
148 circulation which is predicted in the very long-term as a response to climate change^{19,20},
149 but the recent slowdown is likely part of dynamical variability occurring on shorter
150 timescales, it does not imply a change in the general circulation strength. More than year-
151 to-year variability, multiyear periods of age-of-air increase or decrease, as those
152 highlighted in our study or reported recently²¹, will likely complicate the search of a long-
153 term trend in mean circulation.

154 We have presented observations and simulations of a recent HCl increase in the northern
155 hemisphere lower stratosphere. We ascribe it to dynamical variability, occurring on a
156 timescale of a few years, characterized by a persistent slowing of stratospheric circulation
157 after 2005, bringing HCl-enriched air into the NH lower stratosphere. We find no
158 evidence that unidentified SG_{Cl} are responsible for this HCl increase. In the southern
159 hemisphere, a fairly constant decrease has been observed over the last ten years.
160 Globally, our ground-based observations indicate a mean HCl decrease of 0.5%/yr for
161 1997-2011, compatible with the 0.5-1 %/yr range which characterized the post-peak
162 reduction of tropospheric chlorine⁴. Hence, we conclude that the Montreal Protocol is still
163 on track, and is leading to an overall reduction of the stratospheric chlorine loading.
164 However, multiyear variability in the stratospheric circulation and dynamics, as identified
165 here, could lead to further unpredictable increases or redistribution of HCl and other
166 stratospheric tracers. Therefore, such variability and its causes will have to be thoroughly

167 characterized and carefully accounted for when evaluating trends or searching for ozone
168 recovery.

169 **References**

- 170 1. Lovelock, J. E., Maggs, R. J., and Wade, R. J. Halogenated hydrocarbons in and over
171 the Atlantic. *Nature* **241**, 194-196 (1973).
- 172 2. Molina, M. J. and Rowland, F. S. Stratospheric sink for chlorofluoromethanes:
173 chlorine atom-catalysed destruction of ozone. *Nature* **249**, 810-812 (1974).
- 174 3. Farman, J. C., Gardiner, B. G., and Shanklin, J. D. Large losses of total ozone in
175 Antarctica reveal seasonal ClO_x/NO_x interaction. *Nature* **315**, 207-210 (1985).
- 176 4. *Scientific Assessment of Ozone Depletion: 2010, Global Ozone Research and*
177 *Monitoring Project Report N°52* (World Meteorological Organization, 2011).
- 178 5. Rinsland, C. P. *et al.* Long-term trends of inorganic chlorine from ground-based
179 infrared solar spectra: Past increases and evidence for stabilization. *J. Geophys. Res.*
180 **108**, 24235-24249 (2003).
- 181 6. Froidevaux, L., *et al.* Temporal decrease in upper atmospheric chlorine. *Geophys.*
182 *Res. Lett.* **33**, doi:10.1029/2006GL027600 (2006).
- 183 7. Kohlhepp, R. *et al.* Observed and simulated time evolution of HCl, ClONO₂, and HF
184 total column abundances. *Atmos. Chem. Phys.* **12**, 3527-3557 (2012).
- 185 8. Zander, R. *et al.* The 1985 chlorine and fluorine inventories in the stratosphere based
186 on ATMOS observations at 30° north latitudes. *J. Atmos. Chem.* **15**, 171-186 (1992).
- 187 9. Nassar, R. *et al.* A global inventory of stratospheric chlorine in 2004. *J. Geophys. Res.*
188 **111**, doi:10.1029/2006JD007073 (2006).
- 189 10. Gardiner, T. *et al.* Trend analysis of greenhouse gases over Europe measured by a
190 network of ground-based remote FTIR instruments. *Atmos. Chem. Phys.* **8**, 6719-6727
191 (2008).

- 192 11. Froidevaux, L. *et al.* GOZCARDS Merged Data for Hydrogen Chloride Monthly
193 Zonal Means on a Geodetic Latitude and Pressure Grid, version 1.1, Greenbelt, MD,
194 USA: NASA Goddard Earth Science Data and Information Services Center, Accessed
195 June, 2013 at doi:10.5067/MEASURES/GOZCARDS/DATA3002 (2013).
- 196 12. Froidevaux, L. *et al.* Global OZone Chemistry And Related Datasets for the
197 Stratosphere (GOZCARDS): Methodology and Sample Results with a focus on HCl,
198 H₂O, and O₃. Submitted to *Atmos. Chem. Phys.* (2014).
- 199 13. Russell, J. M., III, *et al.* The Halogen Occultation Experiment. *J. Geophys. Res.* **98**,
200 10777-10797 (1993).
- 201 14. Bernath, P. F. *et al.* Atmospheric Chemistry Experiment (ACE): mission overview.
202 *Geophys. Res. Lett.* **32**, doi:10.1029/2005GL022386 (2005).
- 203 15. Waters, J. W. *et al.* The Earth Observing System Microwave Limb Sounder (EOS
204 MLS) on the Aura satellite. *IEEE Trans. Geosci. Remote Sens.* **44**, 1075-1092 (2006).
- 205 16. Laube, J. C. *et al.* Newly detected ozone-depleting substances in the atmosphere.
206 *Nature Geoscience*, doi:10.1038/ngeo2109 (2014).
- 207 17. Dee, D. P. *et al.* The ERA-Interim reanalysis: configuration and performance of the
208 data assimilation system. *Q. J. Roy. Meteorol. Soc.* **137**, 553-597 (2011).
- 209 18. Waugh, D. W., Strahan, S. E., and Newman, P. A. Sensitivity of stratospheric
210 inorganic chlorine to differences in transport. *Atmos. Chem. Phys.* **7**, 4935-4941
211 (2007).
- 212 19. Engel, A. *et al.* Age of stratospheric air unchanged within uncertainties over the past
213 30 years. *Nature Geoscience* **2**, 28-31 (2009).

- 214 20. McLandress, C. and Shepherd, T.G. Simulated anthropogenic changes in the Brewer-
215 Dobson circulation, including its extension to high latitude. *J. Climate* **22**, 1516-1540,
216 (2009).
- 217 21. Stiller, G. P., *et al.* Observed temporal evolution of global mean age of stratospheric
218 air for the 2002 to 2010 period. *Atmos. Chem. Phys.* **12**, 3311-3331 (2012).
- 219 22. Rothmann, L. S. *et al.* The HITRAN 2008 molecular spectroscopic database. *J.*
220 *Quant. Spec. and Rad. Transf.* **110**, 533-572 (2009).

221 **Acknowledgments**

222 The University of Liège contribution was mainly supported by BELSPO and the F.R.S. –
223 FNRS, both in Brussels. Additional support was provided by MeteoSwiss (Global
224 Atmospheric Watch) and the Fédération Wallonie-Bruxelles. We thank the International
225 Foundation High Altitude Research Stations Jungfraujoch and Gornergrat (HFSJG,
226 Bern). The SLIMCAT modelling work was supported by the UK Natural Environment
227 Research Council (NCAS and NCEO). The FTIR measurements at Ny-Ålesund,
228 Spitsbergen, are supported by the AWI Bremerhaven. The work from Hampton
229 University was partially funded under the NASA MEASURE’s GOZCARDS program
230 and the National Oceanic and Atmospheric Administration’s Educational Partnership
231 Program Cooperative Remote Sensing Science and Technology Center (NOAA EPP
232 CREST). The ACE mission is supported primarily by the Canadian Space Agency. We
233 thank U. Raffalski and P. Voelger for technical support at IRF Kiruna. The National
234 Center for Atmospheric Research is supported by the National Science Foundation. The
235 observation program at Thule, GR is supported under contract by the National
236 Aeronautics and Space Administration (NASA) and the site is also supported by the NSF

237 Office of Polar Programs. We thank the Danish Meteorological Institute for support at the
238 Thule. Work at the Jet Propulsion Laboratory, California Institute of Technology, was
239 performed under contract with NASA; the assistance of R. Fuller in producing the
240 GOZCARDS data set is acknowledged, and work by many ACE-FTS, HALOE, and MLS
241 team members who helped to produce data towards the GOZCARDS data set is also
242 acknowledged. We thank O. E. García, E. Sepúlveda, and the State Meteorological
243 Agency (AEMET) of Spain for scientific and technical support at Izana. The Australian
244 Research Council has provided significant support over the years for the NDACC site at
245 Wollongong, most recently as part of project DP110101948. Measurements at Lauder are
246 core funded through New Zealand's Ministry of Business, Innovation and Employment.
247 We are grateful to all colleagues who have contributed to FTIR data acquisition. We
248 thank ECMWF for providing the ERA-Interim reanalyses.

249 **Author contributions**

250 MP, JH, FH, EM, I. Mu., NBJ and CPW, DS performed the Ny-Ålesund, Thule, Kiruna
251 and Izana, Jungfraujoch, Tsukuba, Wollongong and Lauder retrievals for HCl,
252 respectively. PFB and KAW provided ACE-FTS data, LF and JA the GOZCARDS
253 dataset. JA, PFB, LF, JR III and KAW provided expertise on satellite data usage. MPC,
254 RH, SD and WF designed and performed the SLIMCAT runs, sensitivity analyses and
255 transport diagnostics. TR performed the KASIMA model run and corresponding
256 diagnostics. BF and EM performed the trend analyses and compiled the results. JN, MTC,
257 TB, CS, I. Mo. and HN, MS, DWTG and DS are responsible for the instrumentation and
258 data acquisition at the NDACC stations. EM initiated and coordinated the study. The
259 figures were prepared by EM and BF (Fig. 1), EM (Fig. 2), RH and MPC (Fig. 3) and TR

260 (Fig. 4). EM, MPC and JN wrote the manuscript. Together with TR, they revised it and
261 included the comments from the co-authors.

262 **Author information**

263 NDACC data are publicly available at <ftp://ftp.cpc.ncep.noaa.gov/ndacc/station/>,
264 GOZCARDS data at <http://measures.gsfc.nasa.gov/opensap/GOZCARDS/>. The authors
265 declare no competing financial interests. Correspondence and request for materials should
266 be addressed to Emmanuel Mahieu (emmanuel.mahieu@ulg.ac.be).

267 **Figure 1 | Evolution of hydrogen chloride (HCl) in the Earth's atmosphere.** Panel **a**
268 shows the long-term total column time series of HCl at Jungfraujoch (running average
269 with a 3-year integration length, step of 1 month; in red, left scale) and the global total
270 tropospheric chlorine mixing ratio (blue curve, right scale). Lower panels display the
271 running average total column time series (1997-2011) of HCl at Ny-Ålesund (**b**),
272 Jungfraujoch (**c**) and Lauder (**d**), derived from the NDACC-FTIR observations, the
273 standard (green) and S2000 (yellow) SLIMCAT simulations. The thin red lines
274 correspond to the ± 2 standard error of the mean range. Minimum columns are observed in
275 July-2007 at the NH sites (dashed lines).

276

277 **Figure 2 | HCl relative rates of change for eight NDACC sites.** Panel **a** provides the
278 rates of change (%/year) for the 1997-2007 time period (1999-2007 for Thule and Izana,
279 1998-2007 for Tsukuba); panel **b** for 2007-2011. The rates of change were derived from
280 the FTIR and GOZCARDS observational data sets and from the two SLIMCAT
281 simulated time series (see legend for colour code). The error bars correspond to the 2- σ
282 level of uncertainty.

283

284 **Figure 3 | Evolution of stratospheric HCl from satellite observations.** Comparison of
285 merged GOZCARDS satellite HCl observations (by HALOE, ACE, Aura/MLS) with
286 SLIMCAT model runs for NH and SH mid-latitude lower (46 hPa) and upper
287 stratosphere (7 hPa). GOZCARDS monthly means are shown as red dots. Linear fits to
288 the GOZCARDS data and standard SLIMCAT run are displayed as red and green lines,
289 respectively, for periods before and after 2005. The dashed black line shows fits to the
290 S2000 run which assumes no change in circulation. An upward trend is observed in the
291 NH lower stratosphere (**d**) while HCl is decreasing in the southern and northern upper
292 stratosphere (**a, b**).

293 **Figure 4 | Spatial distribution of the HCl concentration and age-of-air changes.**
294 Mean differences of the HCl concentration **(a)** and age-of-air **(b)** between 2010/2011 and
295 2005/2006, as a function of altitude and latitude, derived from the standard SLIMCAT
296 simulation. There is a clear asymmetry between both hemispheres, with correlated
297 patterns between age-of-air and HCl, indicating that the HCl changes over that period are
298 consistent with slower/faster circulation in the NH/SH. **c.** Running averages of the mean
299 age-of-air at 50 hPa (thick/thin curve, integration length of 36/6 months), at the same
300 sites as Fig. 1 (time series at 79°N and 45°S have been shifted vertically by -0.75 yr).

301 **Methods**

302 The ground-based observations were performed at the NDACC sites by solar absorption
303 spectrometry in the infrared spectral region, using Fourier Transform Infrared (FTIR)
304 high-resolution instruments. Observations are recorded under clear sky conditions year-
305 round, except at Ny-Ålesund and Thule, where the polar night prevents measurements
306 between about October and February. The HCl total columns were retrieved with the
307 SFIT-2, SFIT-4 or PROFFIT algorithm in narrow spectral ranges encompassing isolated
308 lines of HCl^{5,7}, generally assuming pressure-temperature profiles provided by the
309 National Centers for Environmental Prediction (NCEP). The GOZCARDS^{11,12} dataset for
310 HCl includes zonal average monthly mean time series of stratospheric mixing ratio
311 profiles merging individual measurements from the HALOE (1991-2005), ACE-FTS
312 (2004 onward) and Aura MLS (2004 onward) satellite-borne instruments. Line
313 parameters from recent HITRAN databases²² were adopted in the spectrometric analyses.
314 We used the SLIMCAT and KASIMA models⁷ to support our investigations. Both used
315 ERA-Interim analyses provided by ECMWF¹⁷, and they provided consistent results for
316 the HCl trends, giving confidence in their robustness. The models contain detailed
317 treatments of stratospheric chemistry and have been extensively used for studies of
318 stratospheric ozone⁷. Stratospheric age-of-air was diagnosed in the model runs using an
319 idealised tracer with a linearly increasing tropospheric mixing ratio. For the S2000
320 SLIMCAT simulation, 6-hourly winds of 2000 were used every year from 2000 onwards.
321 The trend determinations were performed with a bootstrap resampling statistical tool¹⁰,
322 considering all available daily or monthly means (excluding the winter months for the very
323 high-latitude sites) while the model datasets were limited to days with available FTIR

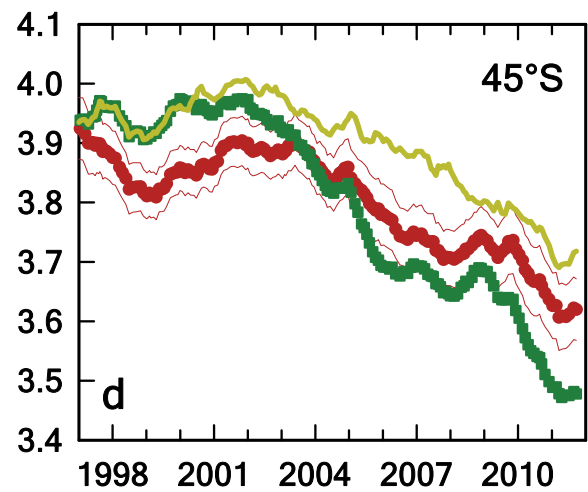
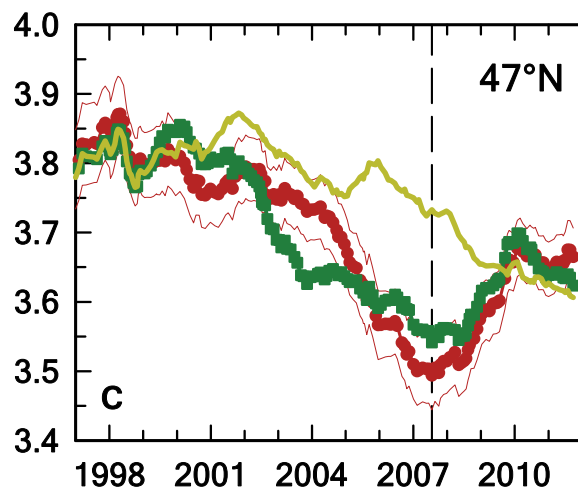
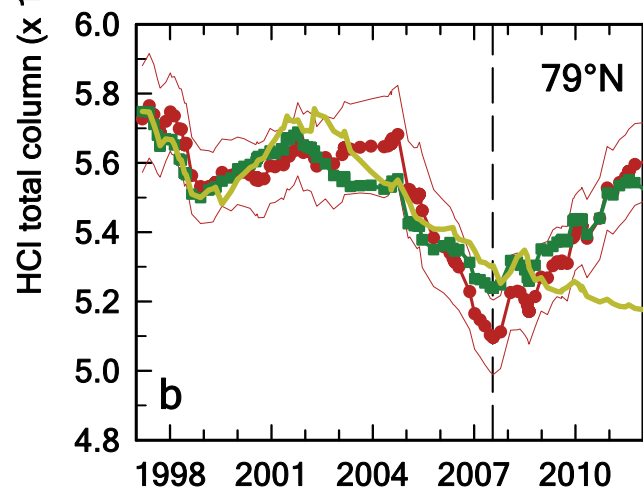
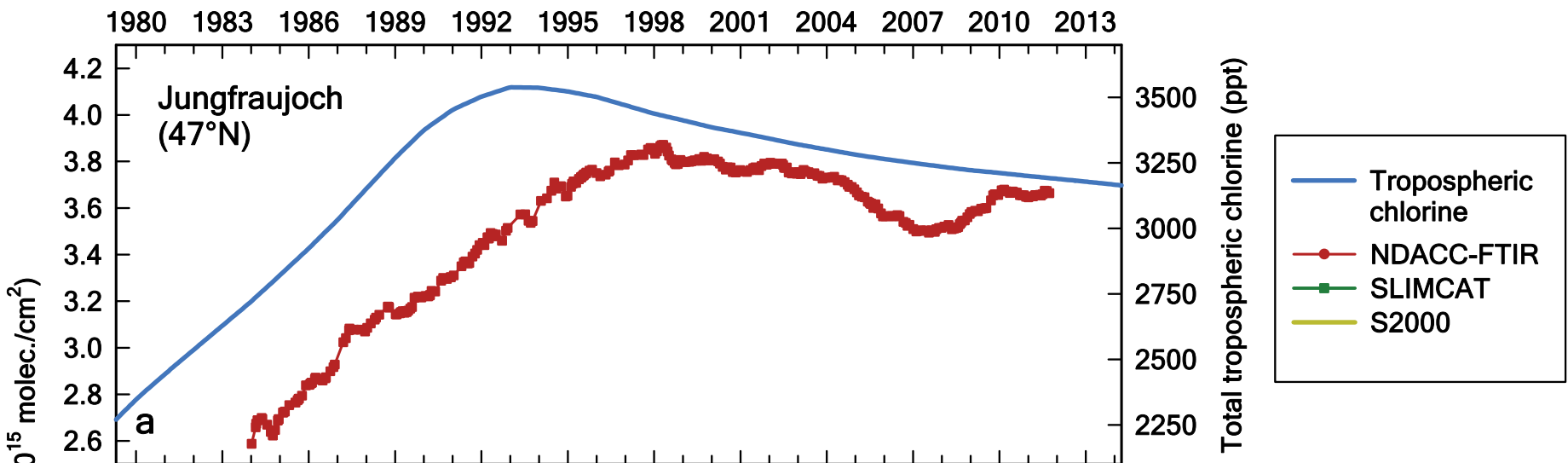
324 measurements. We studied the impact of the FTIR sampling using the bootstrap algorithm,
325 and found no statistically significant impact on the calculated trends.

326 **Extended Data Figure 1 | Evolution of hydrogen chloride (HCl) in the Earth's**
327 **atmosphere and comparison with KASIMA model results.** Panel **a** shows the long-
328 term total column time series of HCl at Jungfraujoch (running average with a 3-year
329 integration length, step of 1 month; in red, left scale) and the global total tropospheric
330 chlorine mixing ratio (blue curve, right scale). Lower panels display the running average
331 total column time series (1997-2011) of HCl at Ny-Ålesund (**b**), Jungfraujoch (**c**) and
332 Lauder (**d**), derived from the NDACC-FTIR observations and from the KASIMA run
333 (grey). The thin red lines correspond to the ± 2 standard error of the mean range. The
334 vertical dashed lines identify the occurrence of the minimum total columns at the NH
335 sites, in July-2007.

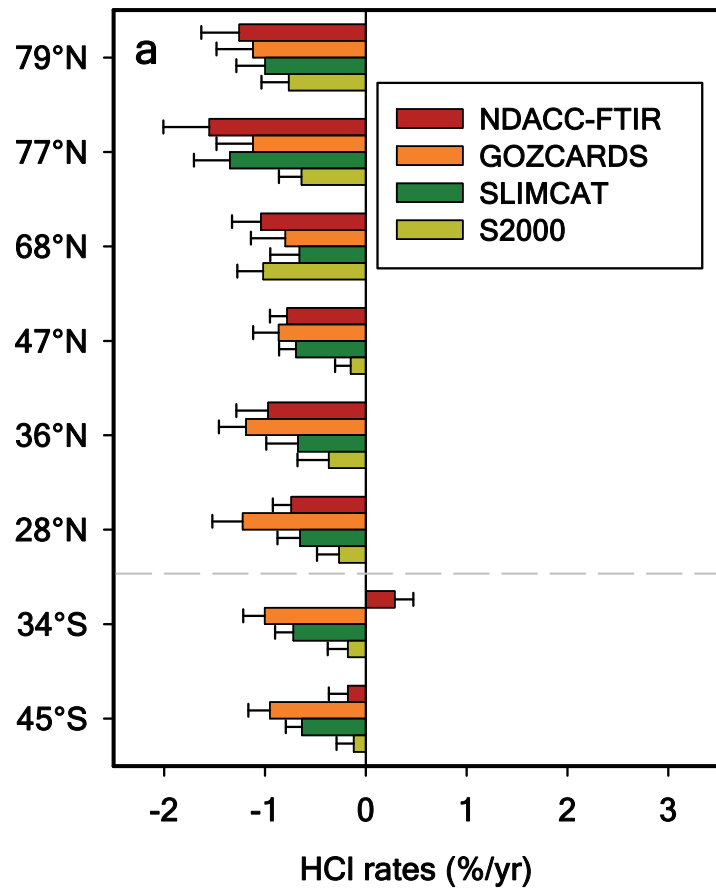
336 **Extended Data Figure 2 | HCl relative rates of change at eight NDACC sites.** The
337 panels **a** and **b** provide the rates of change (%/yr) for the 1997-2007 (1999-2007 for
338 Thule and Izana, 1998-2007 for Tsukuba) and 2007-2011 time periods, respectively.
339 They were derived from the FTIR and GOZCARDS observational data sets and from the
340 SLIMCAT and KASIMA simulated time series (see legend for colour code). The error
341 bars correspond to the 2- σ level of uncertainty.

342 **Extended Data Figure 3 | Evolution of stratospheric HCl from satellite observations.**
343 Comparison of merged GOZCARDS satellite HCl observations (by HALOE, ACE and
344 Aura/MLS) with KASIMA model results for NH and SH mid-latitude lower (46 hPa) and
345 upper stratosphere (7 hPa). GOZCARDS monthly mean observations are shown as red
346 dots. Linear fits to the GOZCARDS data and the KASIMA run are displayed as red and
347 blue lines, respectively, for periods before and after 2005. An upward trend is observed
348 and modelled in the NH lower stratosphere (**d**) while HCl is decreasing in the southern
349 and northern upper stratosphere (**a, b**).

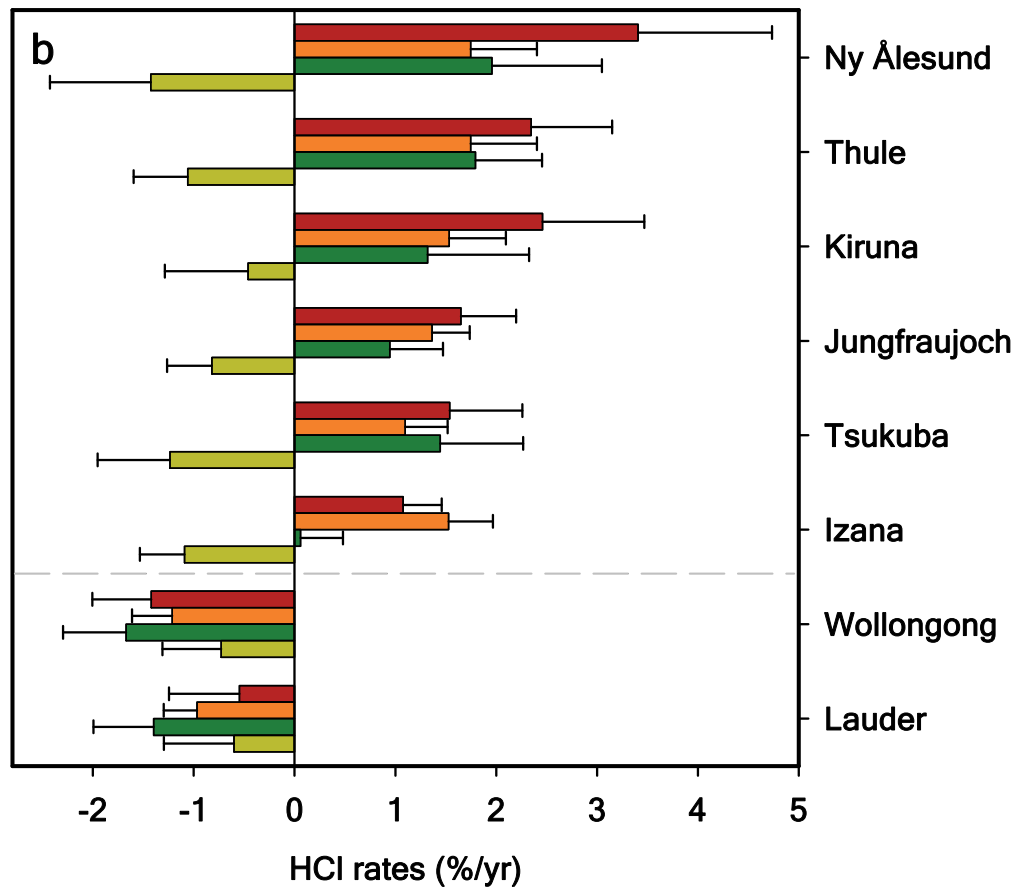
350 **Extended Data Figure 4 | Spatial distribution of the HCl concentration and age-of-**
351 **air changes.** Mean differences of the HCl concentration (**a**) and age-of-air (**b**) between
352 2010/11 and 2005/06, as a function of altitude and latitude, derived from the KASIMA
353 model simulation. **c.** Running averages of the mean age-of-air at 50 hPa (thick/thin curve,
354 integration length of 36/6 months), at the same sites as in Fig. 1 (time series at 79°N/45°S
355 have been shifted vertically by -0.75/-0.50 yr). Comparison with age-of-air time series
356 derived from SLIMCAT (see frame c of Fig. 4) indicates that KASIMA provides higher
357 absolute values of mean age-of-air. Note that the upper boundary of KASIMA is at 120
358 km, yielding higher mean ages, compared to SLIMCAT (upper boundary 60 km).

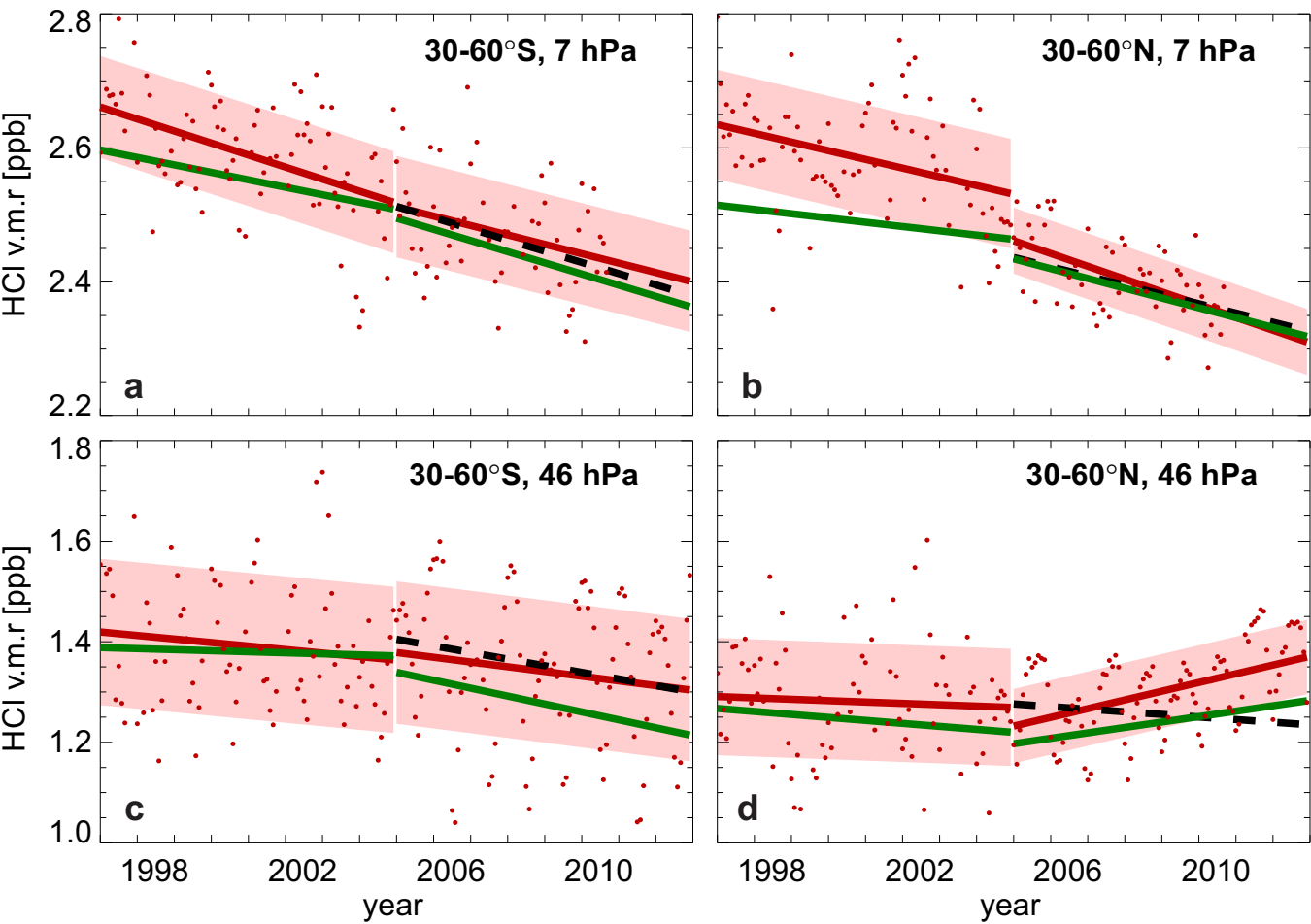


1997-2007

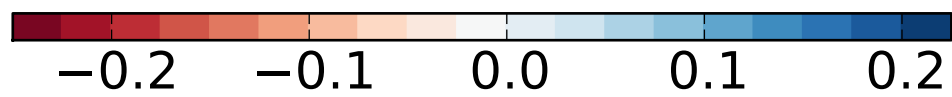


2007-2011





$\Delta\text{HCl conc. (}10^{15} \text{ m}^{-3}\text{)}$



$\Delta\text{Mean age (y)}$

